2023-07

Marine environmental effects on a graphene reinforced epoxy adhered single lap joint between metals and CFRP

Fry-Taylor, R

10.1016/j.ijadhadh.2023.103423
International Journal of Adhesion and Adhesives
Elsevier BV

International Journal of Adhesion & Adhesives 125 (2023) 103423

Contents lists available at ScienceDirect

International Journal of Adhesion and Adhesives

journal homepage: www.elsevier.com/locate/ijadhadh

Marine environmental effects on a graphene reinforced epoxy adhered single lap joint between metals and CFRP

Rudi Fry-Taylor, Maozhou Meng *, Xinyu Wang

School of Engineering, Computing and Mathematics, University of Plymouth, United Kingdom

ARTICLE INFO

Keywords:
Marine environments
Graphene
Single-lap joint
CFRP

ABSTRACT

This study investigates the marine environmental effects on the bonding strength of graphene nanoplatelets (GNPs) reinforced adhesive for a metal/composite single lap joint. Samples were immersed for periods of 1, 2 and 3 weeks in a 50 °C, 3.5% NaCl solution, with the purpose of the heat being the creation of an environment in which simulated an increased ageing period in the joint structure. In a dry condition, the use of GNPs produced a slight increase in lap shear strength of 17% and 14% in the carbon fibre reinforced plastics (CFRP) composite laminate to aluminium and stainless-steel joints respectively. Post immersion, the stainless-steel samples endured 10% less strength degradation than the aluminium samples in the cases with and without GNPs, however the degradation between the same materials with and without GNPs differed less than 2%. On the other hand, the rate at which the materials with GNPs and without GNPs degraded, differed greatly between immersion periods. Mathematical methods were carried out via analytical calculation and FEA modelling, for which values converged with experimental results. The outcomes of these experiments have been the production of highly useful information in terms of material selection and adhesive modification via GNPs for use in the marine environment.

1. Introduction

Where joints between dissimilar materials can be beneficial for reasons from increasing the specific strength to improving anti-corrosive properties – investigations must be carried out perpetually within the field to continually improve the versatility and robustness of the combinations of these materials. The joint of a structure is highly prone to being the initiator of a structural failure, it is said that approximately 70% of structural failures originate from the joint itself [1].

In the case of a single-lap joint, there are multiple methods to achieve such a structure and often it is via mechanical fixing e.g., bolt or rivet. A comparison of riveted and adhesively bonded single-lap joints showed that the bonded structure possessed properties that enabled it to endure ~3.3 times more peak load and absorb ~1.9 times more energy than the riveted joint, with the bonding material being an epoxy adhesive [2]. The efficiency of an adhesive joint is greater than that of a mechanically fixed joint because where there is a high stress concentration in a fixed structure, a bonded structure promotes an even spread of load, eliminating this weakness.

However, an adhered single-lap joint has its shortcomings, such as the defects caused in a joint when placed under conditions replicating that of a marine environment. The water causes plasticization in the joint, which results in a weakening of strength and a lessening of the stiffness within the joint. The most critical damage is due to hydrolysis, breaking down the chemical bonds in the interfacial zone of the joint, developing into displacement of the adhesive [3]. Additionally, a hot and wet environment is a highly prevalent promoter of degradation in the joint, giving strong backing for further investigation with varying materials. The properties of the adherends structure also play a vital role in the overall strength of the joint, with the most important properties to match being those of the thermal and elastic nature – one property specifically being the coefficient of thermal expansion [4,5]. Indeed, the differences in coefficients of thermal expansion of substrates are the causation of large residual stresses in the joint structure [6].

Where an adhered bond in a single-lap joint has clear advantages over a riveted joint for example, there is still much room for improvement. GNPs have shown promising gains in mechanical properties for epoxy resin. For instance, Silva Neto et al. [7] reported lap shearing tests on specimens adhesively joined via a single lap with the addition of graphene in concentrations of 1% and 2% in weight to epoxy adhesive.

* Corresponding author.
E-mail address: maozhou.meng@plymouth.ac.uk (M. Meng).

https://doi.org/10.1016/j.ijadhadh.2023.103423
Received 17 June 2022; Received in revised form 2 May 2023; Accepted 24 May 2023
Available online 2 June 2023

The results showed a failure load increase of 1.27 and 1.58 times, respectively, compared to samples without graphene. It is noted that the amount of graphene in which is added is not necessarily proportional to an increase in mechanical strength, for example, where Guadagno, L et al. [8] reported a ~67% percentage difference increase in tensile strength with addition of 1 wt% graphene oxide (GO), whereas at an addition of 4 wt% GO the strength was reduced by approximately 10%, compared to the 2 wt% GO specimens. This is due to agglomerations of the nanomaterials; an analogous trend is witnessed in research done by Akpinar, I.A. et al. [9], where a 3 wt% graphene modified adhesive performed poorly compared to samples with 1 wt% and 2 wt%. At a higher concentration of filler material there is obviously a higher chance of agglomeration and higher difficulty of dispersion – causing heterogeneity in the adhesive [10–12].

The joining of two dissimilar materials such as CFRP and aluminium or stainless-steel, can often result in detrimental effects to the mechanical properties due to galvanic corrosion [13]. When these materials are placed under water, the water is able to act as an electrolyte – with the more cathodic element of the joint acting as a cathode and the more anodic element acting as an anode, and where this galvanic couple is made with electrical continuity, corrosion will ensue. An effective mitigation of galvanic coupling is to isolate the materials from one another – which can be accomplished via an adhesion layer between the joint. But with the addition of GNPs, there is some controversy between whether corrosion resistance is improved or impaired – evidence has been shown that with an increase of GNPs, comes a decrease in corrosion resistance – especially with additions between 1.5%-3wt% to adhesive due to graphene's high electrical conductivity [4,14]. This would suggest that the resistance to the marine environment will be decreased with the additions of GNPs, which is further investigated in this study in relation to strength degradation.

The reasoning behind the marine environment being an obstacle in the success of an adhesive's longevity is due to the salty solution encouraging the formation of microcavities and micro-cracking, increasing the amount of moisture ingress and promoting hydrolysis of the adhesive, as well as an increase in residual stresses due to swelling [3,15]. These processes result in a weakening of the adhesive's mechanical properties, thus shortening its lifespan. This effect is also reported by Han, X et al. [16], where it is acknowledged that for the higher the salt content in the solution, the higher rate of water diffusion into the adhesive. This is another investigative point, where the amount of mass change due to moisture uptake is reportedly related to the amount of strength degradation, and whether GNPs addition into an adhesive reduces the uptake of moisture.

From comprehensive research, a gap in published reports presented itself in this area of research and experimentation, giving strong support for these experiments and further experiments off the back of this. There is a wealth of research in the strength properties in which the addition of graphene into an epoxy adhesive brings, but coverage on the effects of using graphene in the marine environment are few and far between, particularly with the consideration of different adherends. It is especially important to fill this void because there can be a large contrast in conclusions depending on the specific amount of graphene used, and it is likely that there is an optimal amount depending on the application, whether it be to improve strength, reduce corrosion or reduce moisture uptake, each of these are likely to have differing optimal values. The testing carried out in this study was to investigate whether the nanoplatelet addition affects the adhesive materials resistance to corrosion and degradation, and which metallic adherend performs more positively over time when in adhesion to CFRP in a simulated marine environment. Finite element analysis (FEA) model was also developed to investigate the failure mechanisms.

2. Experiment setup

The metallic adherends used in this study include 1.5 mm stainless steel 304 (SS) and 2 mm aluminium HE9/T6 sheets (Al). CFRP composite laminate was 2 mm plain weave woven manufactured by standard resin transfer moulding (RTM) process, and the fibre volume fraction was 50%. The metallic adherends were cut using a waterjet cutter, with a tolerance of $\pm 0.4mm$, the CFRP adherends were cut using a diamond bladed bench saw with a tolerance of $\pm 0.5mm$. GNPs were in sub-micro power form, supplied by Sigma-Aldrich. The adhesive was marine grade SpaBond 340 LV epoxy, supplied by Gurit. The material properties of these adherends are given in Table 1.

Sample preparation and tensile test procedure were following ASTM D3165, adopting a 0.5 mm adhesive layer and 25 mm overlap [17]. The tensile testing was performed on an Instron 5582 under 1.27 mm/min strain rate. Five repeats were carried out for each configuration, and average was calculated. A jig, with a 0.5 mm bond line clearance was 3D printed to enable an efficient and effective lay-up process. Using a jig, many single lap joints could be configured in a short period of time with the quality of the joint in assurance. Fig. 1 shows the model of the designed jig, and the lapped joint samples.

Surface preparation is essential to the adhesive bonding strength, for example a simple acetone surface wipe-out showed no gain in shear strength at 1 wt% or 2 wt% GNPs within the single lap joint [18], but an adhesive joint between aluminium alloys with 0.42%wt GNPs added resulted in seeing up to a 100% increase in shear strength where samples were grit blasted compared to simply acetone cleaning [19]. Indeed, the adhesive supplier, Gurit [20], recommended grit blasting with fused alumina grit to increase the surface roughness for adhesion preparation, which was also adopted by the present study. Adherends were cleaned with acetone, grit blasted with brown fused alumina grit, and further cleaned with acetone to remove any remaining oils and grease. The surface roughness (Ra) was then measured via Olympus Latex confocal microscopy as shown in Fig. 2. The method of grit blasting not only produced the highest surface roughness measurements in the materials, but also presented the most consistent roughness over the adhesion zone of the three tried methods. For example, acetone cleaning and sanding of the aluminium samples returned an average Ra measurement of 1.6 μm. and 2.3 μm, respectively – whereas grit blasting returned an average Ra measurement of 4.1 μm. The purpose of this measurement is to establish the optimal surface preparation method. Research by Ng, L et al. [21] concluded similar results, where grit blasting the metal specimens resulted in the highest surface roughness measurement compared to other methods.

Preventing agglomerations of the nanomaterial in the adhesive is crucial when attempting to enhance an adhesive with nanomaterials, but it is difficult due to the high viscosity of the adhesive compound. So, as Akpinar, I.A et al. [9] expressed, reducing the viscosity of the epoxy by adding a surfactant to reduce the surface energies, is another way of easing the mixing process. The method in which was adopted for mixing the graphene into the epoxy adhesive for this study was by way of reducing the viscosity of the epoxy adhesive by using acetone, as this can be evaporated once mixed. However, mixing acetone with epoxy causes a strength reduction in the adhesive as explained by Loos, M.R. et al. [22]. For this reason, the acetone treatment (8 wt%) was carried out upon the adhesives with and without the addition of GNPs (1 wt%), thus ensuring consistency between sample groups. On completion of laying up the single-lap joints within the jig, 15 kg clamping force was applied

Table 1
Material properties and dimensions of adherends. SS: stainless steel; Al: aluminium; CFRP: carbon fibre reinforced plastics.

Material	Dimensions (mm)	Young's Modulus (GPa)	Tensile Strength (MPa)	Density (kg/m^3)
SS	100 × 25 × 1.5	190	517	7800
Al	100 × 25 × 2	69	240	2700
CFRP	100 × 25 × 2	70	600	1600
Epoxy	25 × 25 × 0.5	2.8	50	1130

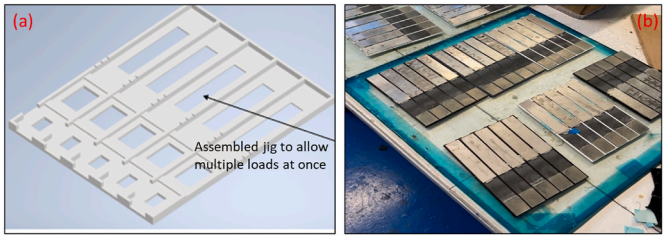

Fig. 1. (a) 3D-printed jig for single-lap joining; (b) cured samples.

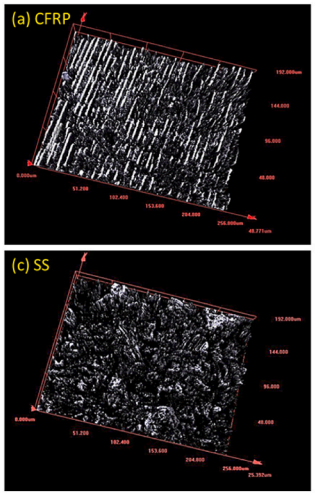

Adherend	Ra (um)
SS	2.4
Al	4.1
CFRP	4.8

Fig. 2. Surface characteristics of the adherends. The Ra values shown in the table were the average of three samples for each adherend.

evenly and on top of samples via a flat glass panel, then the samples were cured at 21 °C for 24 h and post-cured for 16 h at 50 °C.

Four sets of tensile tests were carried out in sequence, corresponding to the immersion period at 0, 1, 2, and 3 weeks. A 3.5% salt water was prepared to simulate the marine environment, and moisture ingress was measured as per instruction of ASTM D5229 [23]. Table 2 gives a summary of the sample configuration and abbreviation. For example, SS0G.0 represents SS-CFRP specimen without GNPs reinforcement in a dry condition, while AL1G.3 means Al-CFRP specimen with 1 wt% GNPs reinforcement after 3-week immersion. Prior to placing samples in the immersed environment, the samples were placed in an oven at 50 °C for 24 h before taking their dry weights and immersing them. Carrying out this process prior to immersion allowed the moisture intake curve to be drawn from dry.

Table 2
Summary of single lap samples. SS0G.0: SS-CFRP without GNPs in dry condition; Al1G.3: AL-CFRP with 1 wt% GNPs after 3-week immersion.

ID	Adherend	Adhesive	GNPs Content	Immersion (days)	Quantity
SS0G.0	SS to	Epoxy	0%	0	5
SS0G.1	CFRP			7	5
SS0G.2				14	5
SS0G.3				21	5
AL0G.0	Al to		0%	0	5
AL0G.1	CFRP			7	5
AL0G.2				14	5
AL0G.3				21	5
SS1G.0	SS to	GNPs	1%	0	5
SS1G.1	CFRP	reinforced		7	5
SS1G.2		epoxy		14	5
SS1G.3				21	5
AL1G.0	Al to		1%	0	5
AL1G.1	CFRP			7	5
AL1G.2				14	5
AL1G.3				21	5

3. Mathematical modelling

In an experimental procedure, where possible, it is important to analyse the system and its states through estimations and hand calculations. In mechanical testing especially, carrying out hand calculations alongside Finite Element Analysis (FEA) can allow predictions and estimations of values to expect from experimental results, alongside that potential failure mechanisms can be spotted out.

The paper by S. Her. [1], proposed a method for carrying out a 2-dimensional analytical analysis for a single lap joint, permitting the calculation of the shear stress along the length of a joint.

$$\tau = \frac{P\lambda}{2}\left(\frac{\cosh(\lambda x)}{\sinh(\lambda l)} - \frac{E_i t_i - E_0 t_0}{E_i t_i + E_0 t_0}\frac{\sinh(\lambda x)}{\cosh(\lambda l)}\right) \quad (1)$$

$$\lambda^2 = \frac{G}{\eta}\left(\frac{1}{E_i t_i} + \frac{1}{E_0 t_0}\right)$$

where G is the shear modulus of adhesive, η is the adhesive thickness, E_i, E_0, t_i, t_0 are elastic moduli and thicknesses of top and bottom of adherends, P is the tensile force per unit length, x is the coordinate along midpoint of overlap area, l is the overlap length. For Gurit SpaBond 340LV epoxy, elastic modulus, shear modulus, tensile strength and shear strength are 2.8 GPa, 1.04 GPa, 50 MPa, and 31 MPa, respectively.

The 3D model of the specimens was drawn in ANSYS Workbench and simulated by ANSYS Mechanical solver [24]. The same physical and mechanical properties were used through analytical and finite element methods. Due to the nature of symmetric geometry, only half of the sample was modelled in ANSYS. A simply supported boundary condition was applied to represent the symmetric features. The displacement on the tap on metal adherend was constrained, while forces corresponding to the maximum tensile force in experiments were applied on the tap on the CFRP adherend. The Mesh of the adhesive layer was refined, specifically a symmetric bias type (bias factor 10) was applied to capture stress distribution closer to the two ends of the adhesive layer, as shown in Fig. 3.

Hygrothermal expansion due to moisture absorption was also considered in the FEA model. The model assumed that moisture content distributes uniformly within both the epoxy adhesive layer and matrix of composite, and the moisture content in different immersion periods was applied on the adhesive layer and composite laminate to investigate the time-dependent shear stress distribution within the adhesive layer. The evaluation of the principal coefficient of hygrothermal expansion of CFRP composite laminate (β_c) was based on the 'rule of mixture' that

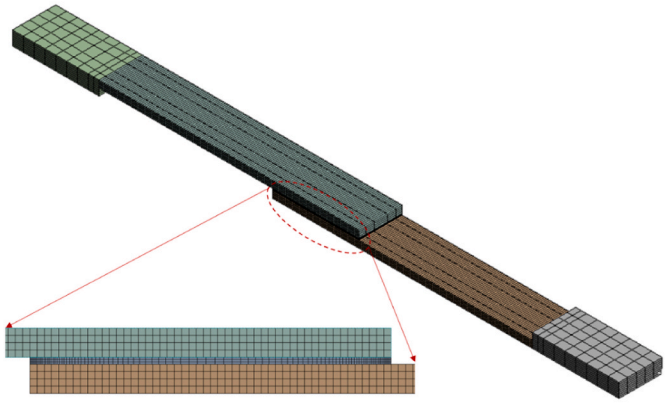

Fig. 3. The mesh of Al-CFRP single lap sample. Only half of the geometry was considered, resulting in approximately 50 k nodes.

was discussed in Refs. [25,26].

$$\beta_c = \frac{E_m}{E_c}\frac{\rho_c}{\rho_m}\beta_m \tag{2}$$

where β_c and β_m are the coefficient of hygrothermal expansion (CHE) of the composite and epoxy matrix; ρ_c and ρ_m are the density of composite and epoxy matrix. E_m and E_c are representative of the young's modulus of the matrix and the composite, respectively.

The moisture content of the epoxy adhesive (M_a) and CFRP composite laminate (M_c) can be calculated by the ratio of masses of each material in the lap joint. In this study, the coefficient of hygrothermal expansion of epoxy adhesive β_a is assumed to be the same as β_m, which has been measured as 0.22 by Vanlandingham, M.R. et al. [27], therefore β_c is calculated as 0.012 from Equation (2). Note that the hygrothermal expansion in transverse direction wasn't considered here because this is free expansion that has no induced residual stress.

4. Results and discussions

4.1. Water uptake

Fig. 4 presents the measured moisture uptakes of the samples across the measured instances. The x-axis is plotted as square root scale, as per Fick's law of diffusion. A clear trend of water uptake can be observed from the figure with the increase of immersion period. With or without GNPs addition, there was only a small difference in the amount of moisture in which both the stainless-steel and aluminium samples took on across all immersion periods. It should be noted that the Al-CFRP specimens showed considerably more moisture content than the SS-CFRP specimens. This is due to the lower density of aluminium, while the water uptake measurement was performed for the single lap specimen as a whole, but only epoxy absorbed moisture.

These water uptake curves were still in the linear stage, which is ahead of the saturation due to the limited immersion period. The slope at this linear stage can be used to calculate the moisture diffusivity. Arrhenius equation (Equation (3)) can be used to interpret the immersion time between room temperature (20 °C) and elevated temperature (50 °C).

$$D = D_0 e^{-\frac{E_a}{RT}} \tag{3}$$

where D_0 is the diffusivity at reference temperature, E_a is the activation energy, R is the gas constant (8.31 $JK^{-1}mol^{-1}$), T is the elevated temperature. As for a rough estimation, diffusivity doubles its speed when the temperature increases 10 °C for most polymer systems.

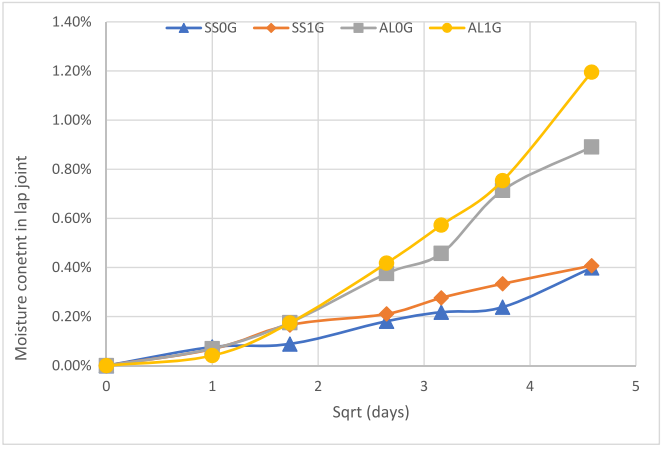

Fig. 4. Moisture uptake across immersion time. The GNPs modified samples absorbed slightly more moisture than those without GNPs. The horizontal axis is plotted in square root scale.

The function of the Arrhenius equation inspired the heightened temperature of immersion, where an increase in temperature in this formula results in an increased diffusivity. Where time for the experiments were limited – an increased diffusivity of the adhesive created a simulated accelerated ageing effect. According to Kahraman, R et al. [15], the diffusivity of an epoxy adhesive whilst at 20 °C in a 3.5% NaCl solution, is $6.5 \times 10^{-8} mm^2/s$. Whereas at 50 °C, Han, X et al. [16] reported the value at approximately $7.5 \times 10^{-7}\ mm^2/s$ – this is an increase of 11.6 times. This is also related in the work from Heide-Jørgensen, S et al. [28], where an Arrhenius relationship in the diffusion of epoxy adhesive correctly simulates the diffusion rate by temperature of the environment.

From Tables 1 and it can be calculated that the weight percent of epoxy adhesive is approximately 9% of that within the CFRP composite laminate as matrix. Considering the density ratio of SS/carbon/epoxy and Al/carbon/epoxy, fibre volume fraction, and assuming the densities of the epoxy adhesive and epoxy matrix are the same, the moisture uptake within epoxy (both adhesive and composite matrix) should be multiplied by 10.9 and 6.3 in SS-CFRP and Al-CFRP samples respectively, and the results are shown in Fig. 5, giving a relatively linear trend for these four sets of specimens. Though these moisture uptake curves have not reached the plateau, the absolute value of moisture content within epoxy resin was at a high level, exceeding the saturation limit of 2–4% [27,29,30], therefore, it is assumed that the moisture content was saturated in the current study and longer immersion period is unnecessary.

4.2. Lap shear strength

The bonding strength of the single lap joint was characterised by lap shear strength. The average lap shear strength can be calculated by using the overlap area of the adhesion zone for each sample and the failure load as shown in Equation (4).

$$\tau = \frac{F}{A} \tag{4}$$

where F is the tensile force at failure point, and A is the overlap area.

Fig. 6 shows the average lap shear strength of control samples (without immersion). The shear stresses endured by the Al-CFRP and SS-CFRP samples with the addition of 1%wt GNP were that of a percentage difference increase of 17% and 14%, respectively, compared to their counterpart with 0%wt GNP in the adhesive.

Though less drastic, these results support those of Xue, G et al. [5] where a 1%wt of graphene increased the lap shear strength of the specimen by 56%. With both the graphene modified and non-Graphene modified adhesive, the SS-CFRP sample withheld a higher shear stress value by 27% and 30%, respectively, to its Al-CFRP specimen

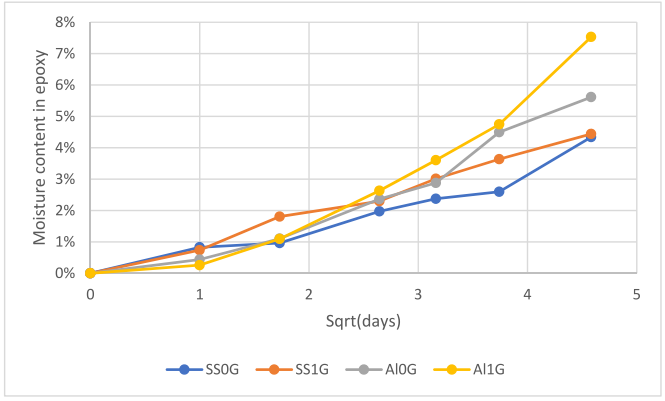

Fig. 5. Moisture uptake within epoxy. Epoxy adhesive layer is assumed to be the same as the epoxy matrix within CFRP composite laminates.

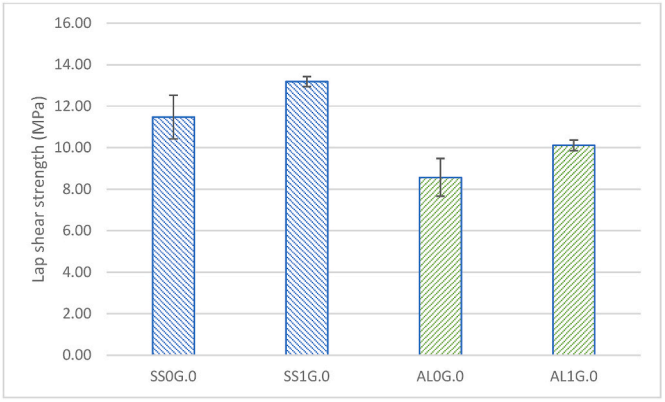

Fig. 6. Lap shear strength of dry specimens of SS-CFRP and AL-CFRP. 17% and 14% lap shear strength increase were obtained after 1 wt% GNPs was added. Standard deviation is also plotted in the chart.

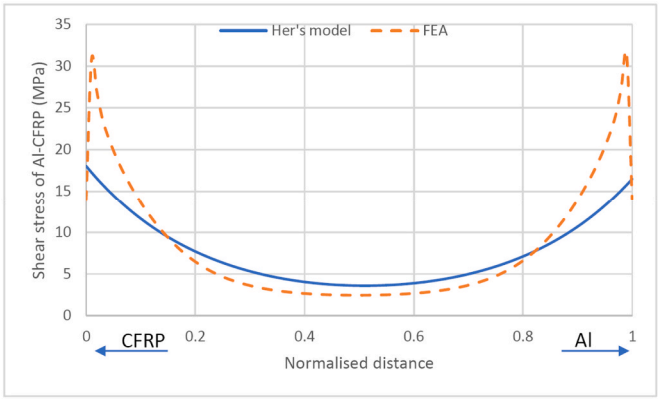

Fig. 8. Normalised lap shear stress distribution along the adhesive layer (Al-CFRP)).

counterpart. Though with consideration to the specimen's mass, the SS-CFRP joint is 55% heavier than that of the aluminium joint.

Apparently, the calculation from Equation (4) assumes that the shear stress distributes uniformly across the whole adhesive layer. This is reasonable for a quick evaluation of the bonding strength. However, a closer look into the stress distribution is necessary to understand the failure mechanism of the lap joint. Figs. 7 and 8 displays the shear stresses of SS-CFRP and Al-CFRP samples along the length of the joint in the FEA model, compared against S.Her's model. Both models return very similar shear stresses at two ends of the lap joint, in both SS-CFRP and Al-CFRP joints, however extremely high stress peaks were spotted out near the edge of the adhesive joint from the FEA model, which is the so-called edge effects. Similar edge effects in 3D FEA modelling of laminated composites have been discussed in Ref. [31].

Experimentally, the SS-CFRP samples endured 28.9% more shear stress than Al-CFRP samples in the current study; numerically, the SS samples endured 28.5% more shear stress than Al-CFRP samples – the shear strength increase from Al-CFRP to SS-CFRP also converges from numerical to experimental analysis. Taking the average value of shear stresses along the two single lap joints from both FEA and S.Her's models, the values were very close to the calculation from Equation (3), however these values (in the order of 10 MPa) are well below the adhesive shear strength (31 MPa). Therefore, it is believed that the failure of the single lap joints was due to the edge effects that create significantly higher stress close to the edge of the adhesive layer, and a 3D FEA model can apparently provide much more details of the stress distribution. Though S.Her's model predicts an elevated stress near the edge, these edge effects are still underestimated. It should be noted that the stress distribution of Al-CFRP joint is relatively symmetric due to the similar elastic moduli of the two adherends, however the shear stress near stainless steel adherend is considerably higher than the stress in the stainless steel adherend due to a higher modulus of stainless steel, and it can be expected that failure initiated from the contact area between the adhesive and CFRP composite laminate. In this point of view, extra care should be taken to protect the adhesive layer near the adherend with a lower modulus if joining dissimilar materials.

4.3. Stress degradation

Once immersed, detriment is caused to the reliability and consistency of the samples with GNP addition. The addition of GNPs in a dry condition resulted in an increase in peak failure load, and a higher consistency (lower standard deviation) in the measured values was observed. However, this improvement was observed to have been lost after the first immersion period (7 days) in the 50 °C, 3.5% NaCl solution. This is illustrated in Figs. 9 and 10, where the measured failure load decreased dramatically.

A similar relationship is drawn when comparing the results of the GNPs modified samples of both SS-CFRP and Al-CFRP to their non-GNPs equivalents. The degradation of the GNP modified samples appears to arise at a greatly accelerated rate in the first immersion period of 7 days. In this same period, the GNP modified SS-CFRP and Al-CFRP samples absorbed a percentage difference of 15%, and 10% more moisture than their non-GNPs counterparts - as observed in Fig. 4. Similar phenomenon has been reported by Han, X et al. [16], where it is believed that a higher water uptake resulted in further weakening of the joint, a hypothesis for which is supported in the first immersion period. However,

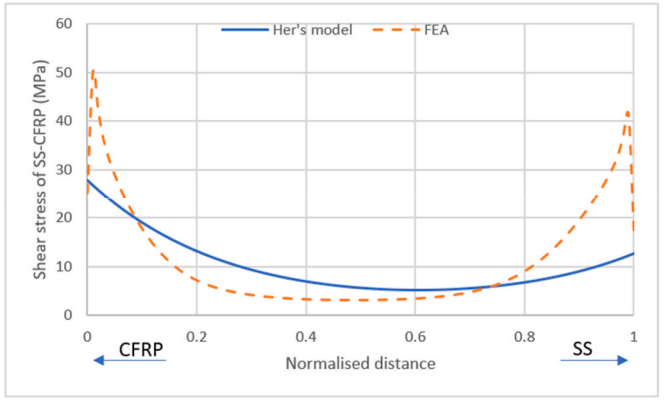

Fig. 7. Normalised lap shear stress distribution along the adhesive layer (SS-CFRP). SS adherend is on left while CFRP on right.

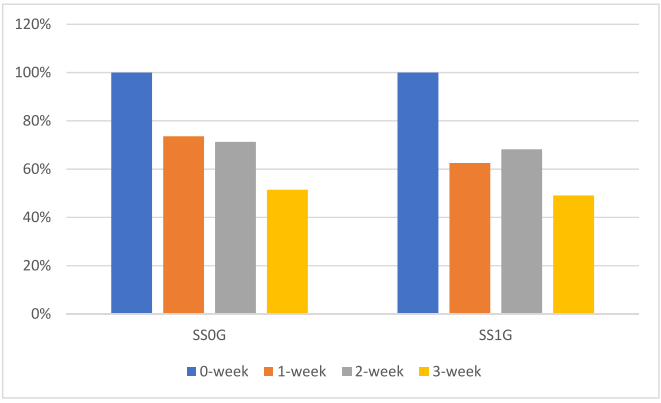

Fig. 9. Lap shear strength degradation of SS-CFRP samples in a marine environment. The stresses have been normalised to the dry condition.

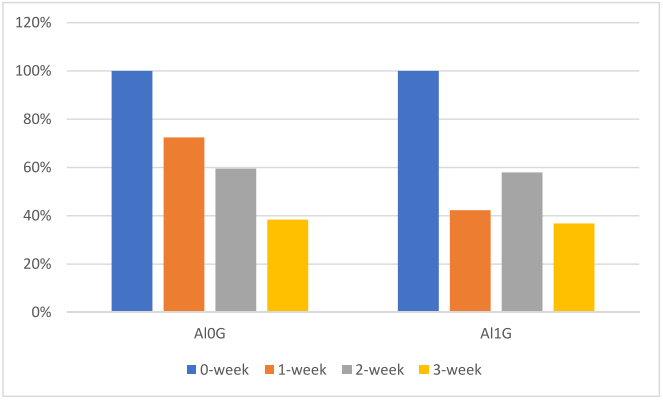

Fig. 10. Lap shear strength degradation of Al-CFRP samples in a marine environment. The stresses have been normalised to the dry condition.

an interesting analysis is that between 7 and 14 days, the lap shear strengths of both the GNPs sample groups regained strength whilst still taking on moisture. Whereas the rate at which the non-GNPs samples' strength degraded was slowed in this period, but they continued to lose strength. This finding is to be further researched.

After 3-week immersion, the total degradation of the samples between GNPs and non-GNPs differed by 2.4% and 1.7% for SS-CFRP and Al-CFRP, respectively – in favour of the non-GNPs samples in both cases. Where there was little difference in moisture uptake of SS-CFRP samples with and without GNPs, the Al-CFRP samples with GNPs took on a percentage difference of 30% more moisture than the non-GNP samples, but the difference in lap shear strength degradation was just 1.7% over the entire immersion period. This suggests that the moisture uptake is not a direct cause of strength degradation in this environment; and that there is no improvement in lap shear strength when using GNPs in adhesion at an addition of 1%wt under marine environmental conditions – analogous with the conclusions of [14].

This decrease in strength and consistency in the material properties within the GNPs samples can be hypothesised to be a result of higher corrosion, where the GNPs were facilitating higher conductive properties upon the epoxy adhesive. Kopsidas, S et al. [14] reported that the addition of GNPs in an epoxy adhesive is only beneficial for preventing corrosion when used at lower loadings ($\leq$0.5%wt), whereas at a higher addition of the nanomaterial into an epoxy adhesive, an electrically conductive coating is created due to the GNPs high electrical conductivity, thus promoting corrosive currents through the adhesive, increasing the corrosive effects, and thus lessening the strength. It is recommended by Vargal, C [32]. that joints where dissimilar metals (i.e. Aluminium and CFRP) and an electrolyte (seawater) are present, loading the joint structure with graphitic material should be avoided as galvanic corrosion is highly promoted due to the electrical conductivity of the filler material. Where the corrosion ensues, non-uniform defects such as micro-cracking and hydrolysis are likely to occur upon the interfacial bond between the adhesive and adherends, as Hirulkar, N et al. [3] denoted, thus causing a wider variety of results.

A joint between CFRP and a metallic adherend is subject to galvanic corrosion. Out of water, Pramanik, A et al. [4] suggest that this reaction is alleviated where there is a non-conductive adhesive layer between the adherends, whereas when in the aqueous environment, the water acts as an electrolyte putting the dissimilar electrodes (dissimilar adherends) in contact electrochemically, with one acting as an anode and one as a cathode [33,34], otherwise known as galvanic coupling. This information suggests that in the marine environment, a joint between SS304 and carbon fibre would degrade less in strength properties. due to factors of galvanic corrosion than an aluminium and carbon fibre joint, to which the experimental results agree at all immersion periods.

4.4. Galvanic effects

The failure modes of the dry samples were dominantly adhesive failure, though for both SS-CFRP and the Al-CFRP samples without GNP there was 1 mixed failure per these groups. As a contrast, soaked samples failed by weakened interface between adhesive layer and metallic adherends. Shown in Fig. 11 are some typical images of the edges of the adhered zone after destructive testing post 3-week immersion for the four sets of samples.

In the images of the Al-CFRP samples (Fig. 11 c-d), both groups are visually discoloured and possess signs of galvanic corrosion, where localised areas present shinier than the rest of the material and pitting corrosion, as when this occurs on aluminium it is relatively visually available on the surface after experiencing the marine environment. Vargel, C [32] explains that the pitting is covered over by white gelatinous pustules of which are Alumina gel '$Al(OH)_3$'. It is these formations which support a qualitative assessment of an increased corrosion rate. The samples with 1%wt GNP within the adhesive appear more affected by this than samples without GNP addition.

Similar details are shown in Fig. 11 a-b comparing the visual corrosive effects on the surface of the stainless-steel materials, depending on whether the group had GNPs added to the adhesive layer or not. In both of the groups of samples, the discolouration is greatly milder than in the aluminium specimens, but areas of corrosion can be seen. Local areas of visually identifiable corrosion are likely the meeting point of the anodic part of the galvanic corrosion that occurs between CFRP and SS in this electrochemical mechanism. Upon visual inspection, it appears that the SS samples with GNP's experienced a higher rate of corrosion. It is also observed from Fig. 4 that there was only a marginal difference in the amount of moisture absorbed by the joint (0.4% vs 0.41%) for non-graphene and graphene modified versions, respectively. This plays against the hypothesis of water absorption being directly related to strength degradation by Han, X et al. [16] as a factor that is ignored in the mentioned analysis is the correlation of the corrosion rate of the materials, for which the present paper identifies.

Throughout both aluminium and stainless-steel groups, the amount of corrosion present on the specimens visually, suggests a higher rate of corrosion in the GNPs modified samples when immersed in the simulated seawater solution. The experimental data concluded with the same reasoning – GNPs at a 1%wt to epoxy is not beneficial to a joint when used in adhesion under marine environmental conditions.

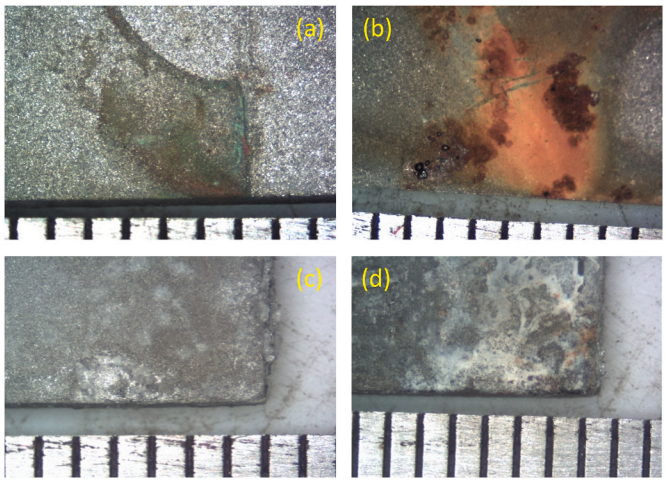

Fig. 11. Typical images of fracture surface on metallic adherends post-immersion. (a) SS0G; (b) SS1G; (c) Al0G; (d) Al1G. A steel rule is showing millimetres for scale of the specimens.

4.5. Hygrothermal effects

Another factor in which the differences of the materials used in the joint are indicated to influence degradation, is in the differences in the adherends coefficient of thermal expansion (CTE) and coefficient of hygrothermal expansion (CHE). Both stainless steel and aluminium have a positive CTE, while it is widely recognised that carbon fibre is CTE negative if not zero. On the other hand, metals and carbon fibre have no water uptake while epoxy expands after moisture diffusion. This difference in the adherends CTE and CHE is reported as a cause of large residual stresses and issues in causing the joint to be unbalanced resulting in adverse effects in the strength of the joint when under hygrothermal conditions [6,35].

Though there was an elevated temperature environment in the immersion, the tensile tests were performed at room temperature, which was the same as the dry samples. Therefore, only hygrothermal effects were considered in the FEA model. Figss. 12 and 13 show the comparison of shear stress distribution of SS-CFRP and Al-CFRP samples in dry and wet (3-week soaked) conditions.

Shown in Figss. 14 and 15 are the evaluation of re-distribution of shear stress with the increase of immersion period. A clear pattern is observed through Figss. 12–15, where more time spent immersed ensued a less distributed spread of shear stress along the length of the joint, due to an increase of shear stresses through the joints mid-section. In a dry condition, the edge effects as discussed in Ref. [31] result in a peak of shear stress at either ends of the adhered zone, which are much greater than the midpoint due to minimal residual stresses where there is no moisture content. Whereas where time spent in water is increased, an escalation of residual stresses is visualised - this is further realised by comparison of minimum and maximum shear stresses across the joint where the peak value due to edge-effects stays relatively static, increasing the net shear stress in the joint. In the aluminium samples 'Week 0', the location of the edge-effect phenomena experienced 13 times the shear stress of the midpoint of the joint, whereas in 'Week 3' the shear stresses at the peak were just 1.6 times greater than the trough (midpoint). The stainless-steel samples experience a corresponding trend, where the peak in 'Week 0' is also 13 times greater than the midpoint, but by 'Week 3' it is just 2.6 times greater.

It is important to establish that this reduction in difference is solely due to an increase in stress around the midsection of the joint, where the already highly stressed regions at each end stay relatively similar throughout the immersion. It is also important to understand that where the dissimilar materials of SS and CFRP having greatly differing elastic moduli resulted in greatly differing shear stresses depending on the end of the joint in question does not follow through to the increase in residual stresses – as the increase in stresses due to the hygrothermal effects is uniform along the mid-section, regardless of the adjoining material.

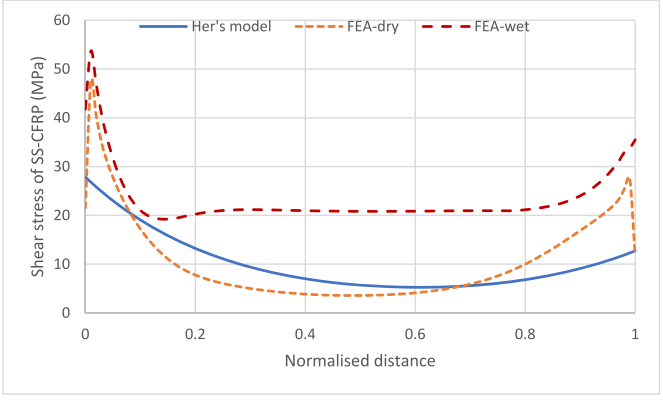

Fig. 12. Comparison of shear stress distribution of SS-CFRP sample in dry and 3-week-soaked conditions.

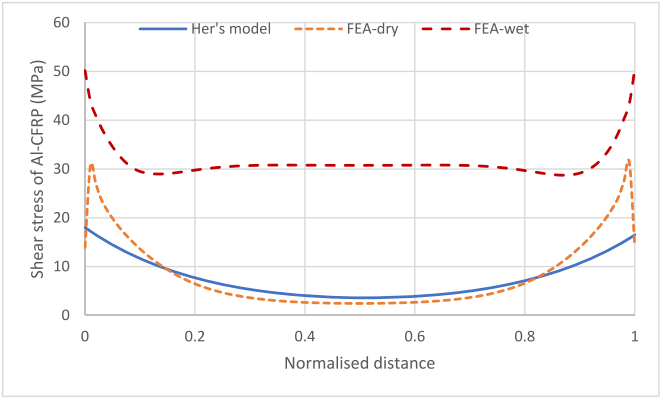

Fig. 13. Comparison of shear stress distribution of Al-CFRP sample in dry and 3-week-soaked conditions.

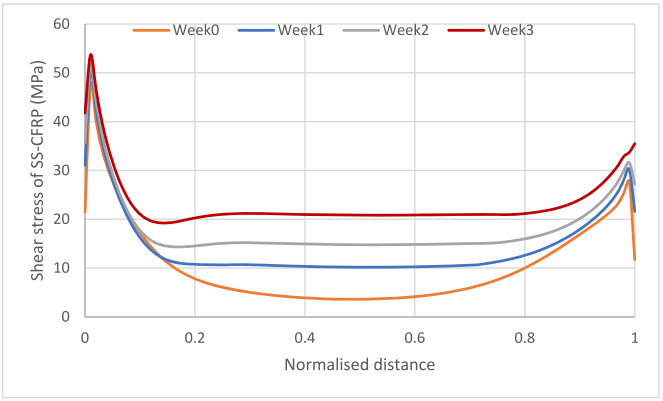

Fig. 14. Time-dependent shear stress distribution of SS-CFRP sample.

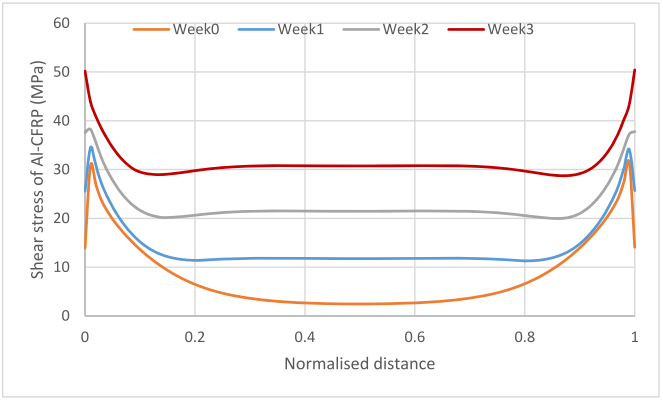

Fig. 15. Time-dependent shear stress distribution of Al-CFRP sample.

Where in the dry samples, the net shear stress was highly influenced by the so-called edge effects – once immersed, the hygrothermal effects cause a build-up of residual stresses, increasing the net shear stresses in the joint, where the only variable is the time spent immersed. It is hypothesised that these hygrothermal effects resulting in an increase of minima shear stresses is causation of detriment to the joints structure, resulting in a much-lessened shear strength. This is parallel to the results of the experiment, where more time spent immersed was followed by a greater degradation of shear strength.

5. Conclusions

This paper investigates the marine environmental effects on the lap shear strength of GNPs modified epoxy adhesive single lap joint for metallic to CFRP composite adherends, by means of experimental, analytical and FEA methods. Some conclusions can be drawn based on this study.

In a dry condition, the addition of GNPs positively affected the strength properties in both the SS-CFRP and Al-CFRP samples. Lap shear strength of SS-CFRP and Al-CFRP joints increased 17% and 14% respectively in this study. However, in all immersed conditions, GNPs modified adhesive specimens performed worse in strength properties in comparison to their non-GNPs counterparts. It was observed that the standard deviation of these immersed samples showed a negative effect on the material properties, meaning that immersion magnified the manufacturing defects.

Based on literature and these experiments, it is not absolute that GNPs enhance or impair a material's resistance to corrosion as an encompassing statement, as it is likely that this is dominantly based on the specific amount in which is added – for which further research is necessary to accurately model the amount. However, in this case a 1 wt % GNP modified epoxy adhesive appears to influence a decrease in corrosion resistance properties.

The addition of GNPs did not affect the moisture uptake in the SS-CFRP samples, whereas in Al-CFRP samples the saturated moisture content was increased by approximately 25%. As a result, the lap shear strength of Al-CFRP samples was also degraded more than SS-CFRP samples. However, the apparent corrosion rate of SS-CFRP samples was more severe.

It was found that shear stress was asymmetrical in the single lap joint with dissimilar adherends, in which higher shear stresses appeared toward the end with lower modulus. Combined with edge effects, extra care should be taken to protect the adhesive layer near the adherend with lower modulus if joining dissimilar materials.

Significant edge effects were unveiled from the 3D FEA results. With the increase of moisture content, the peak shear stress near the edges remained at the same level as dry condition, however the shear stress increased tremendously across the whole adhesive layer. It is concluded that failure initialised from the edges of the adhesive layer in dry samples, while simultaneous debonding was the failure mode of the soaked samples.

Declaration of competing interest

The authors declare that they have no known competing financial interests or personal relationships that could have appeared to influence the work reported in this paper.

Data availability

Data will be made available on request.

Acknowledgement

This work is supported by SuperGen ORE Hub under the early career researcher (ECR) scheme. The authors would also like to thank Dr Jeremy Clark for the support of mechanical testing, Mr Neil Fewings for the support of sample cutting.

References

[1] Her S-C. Stress analysis of adhesively-bonded lap joints. Compos Struct 1999;47 (1–4):673–8.
[2] Chen Y, et al. Mechanical behavior and progressive failure analysis of riveted, bonded and hybrid joints with CFRP-aluminum dissimilar materials. Thin-Walled Struct 2019;139:271–80.
[3] Hirulkar N, et al. Effect of hygrothermal aging and cyclic thermal shocks on the mechanical performance of single-lap adhesive joints. Int J Adhesion Adhes 2020; 99:102584.
[4] Pramanik A, et al. Joining of carbon fibre reinforced polymer (CFRP) composites and aluminium alloys–A review. Compos Appl Sci Manuf 2017;101:1–29.
[5] Xue G, et al. Morphology, thermal and mechanical properties of epoxy adhesives containing well-dispersed graphene oxide. Int J Adhesion Adhes 2019;88:11–8.
[6] Liljedahl C, et al. Modelling the environmental degradation of adhesively bonded aluminium and composite joints using a CZM approach. Int J Adhesion Adhes 2007;27(6):505–18.
[7] Silva Neto A, Cruz DTLd, Ávila AF. Nano-modified adhesive by graphene: the single lap-loint case. Mater Res 2013;16(3):592–6.
[8] Guadagno L, et al. Graphene-based structural adhesive to enhance adhesion performance. RSC Adv 2015;5(35):27874–86.
[9] Akpinar IA, et al. Experimental analysis on the single-lap joints bonded by a nanocomposite adhesives which obtained by adding nanostructures. Compos B Eng 2017;110:420–8.
[10] Prolongo S, et al. Advantages and disadvantages of the addition of graphene nanoplatelets to epoxy resins. Eur Polym J 2014;61:206–14.
[11] Tang L-C, et al. The effect of graphene dispersion on the mechanical properties of graphene/epoxy composites. Carbon 2013;60:16–27.
[12] Sadigh MAS, Marami G. Investigating the effects of reduced graphene oxide additive on the tensile strength of adhesively bonded joints at different extension rates. Mater Des 2016;92:36–43.
[13] Wu X, et al. Investigation on galvanic corrosion behaviors of CFRPs and aluminum alloys systems for automotive applications. Mater Corros 2019;70(6):1036–43.
[14] Kopsidas S, et al. Examining the effect of graphene nanoplatelets on the corrosion resistance of epoxy coatings. Int J Adhesion Adhes 2021;104:102723.
[15] Kahraman R, Al-Harthi M. Moisture diffusion into aluminum powder-filled epoxy adhesive in sodium chloride solutions. Int J Adhesion Adhes 2005;25(4):337–41.
[16] Han X, et al. Characterisation of moisture diffusion and strength degradation in an epoxy-based structural adhesive considering a post-curing process. J Adhes Sci Technol 2018;32(15):1643–57.
[17] ASTM-D3165. Standard test method for strength properties of adhesives in shear by tension loading of single-lap-joint laminated assemblies. 2014.
[18] Nascimento Jr H, et al. An investigation on industrial adhesive nano-modified by graphene nanoplatelets under extreme environmental conditions. Int J Adhesion Adhes 2021;111:102982.
[19] Pawlik M, Lu Y, Le H. Effects of surface modification and graphene nanoplatelet reinforcement on adhesive joint of aluminium alloys. Int J Adhesion Adhes 2020; 99:102591.
[20] Gurit. Sparbond 340LV HT high Tg structural epoxy adhesive. 2021. https://www.gurit.com/-/media/Gurit/Datasheets/spabond-340lv-ht.pdf.
[21] Ng L, et al. The effects of bonding temperature and surface roughness on the shear strength of bonded aluminium laminates using polypropylene based adhesive. J Adv Manuf Technol 2019;13(2).
[22] Loos MR, et al. The effect of acetone addition on the properties of epoxy. Polímeros 2008;18(1):76–80.
[23] ASTM-D5229. Standard test method for moisture absorption properties and equilibrium conditioning of polymer matrix composite materials. 2010.
[24] ANSYS. ANSYS reference manual. 2022.
[25] Clyne TW, Hull D. An introduction to composite materials. Cambridge university press; 2019.
[26] Gibson RF. Principles of composite material mechanics. CRC press; 2016.
[27] Vanlandingham M, Eduljee R, Gillespie Jr J. Moisture diffusion in epoxy systems. J Appl Polym Sci 1999;71(5):787–98.
[28] Heide-Jørgensen S, Ibsen CH, Budzik MK. Temperature dependence of moisture diffusion in woven epoxy-glass composites: a theoretical and experimental study. Mater Today Commun 2021;29:102844.
[29] Pérez-Pacheco E, et al. Effect of moisture absorption on the mechanical behavior of carbon fiber/epoxy matrix composites. J Mater Sci 2013;48(5):1873–82.
[30] Meng M, et al. Effects of hygrothermal stress on the failure of CFRP composites. Compos Struct 2015;133:1024–35.
[31] Meng M, et al. 3D FEA modelling of laminated composites in bending and their failure mechanisms. Compos Struct 2015;119:693–708.
[32] Vargel C. Corrosion of aluminium. Elsevier; 2020.
[33] Hack H. *2.07–Galvanic corrosion.* Shreir's corrosion. Oxford: Elsevier; 2010. p. 828–56.
[34] Abbott R. Analysis and design of composite and metallic flight vehicle structures. Collingwood, ON, Canada: Abbott Aerospace SEZC Ltd.; 2016.
[35] Dominguez F, Carral L. A review of formulations to design an adhesive single-lap joint for use in marine applications. Brodogradnja: Teorija i praksa brodogradnje i pomorske tehnike 2020;71(3):89–119.